minerals

Article

Geochemistry and Mineralogy of Tuff in Zhongliangshan Mine, Chongqing, Southwestern China

Jianhua Zou [1,2,*], Heming Tian [2] and Tian Li [2]

[1] College of Geosciences and Survey Engineering, China University of Mining and Technology (Beijing), Beijing 100083, China

[2] Chongqing Key Laboratory of Exogenic Mineralization and Mine Environment, Chongqing Institute of Geology and Mineral Resources, Chongqing 400042, China; heming1986824@126.com (H.T.); lt_litian@163.com (T.L.)

* Correspondence: zoujianhua1200@gmail.com; Tel.: +86-23-8831-6044

Academic Editors: Shifeng Dai and Thomas N. Kerestedjian
Received: 30 January 2016; Accepted: 11 May 2016; Published: 20 May 2016

Abstract: Coal-bearing strata that host rare metal deposits are currently a hot issue in the field of coal geology. The purpose of this paper is to illustrate the mineralogy, geochemistry, and potential economic significance of rare metals in the late Permian tuff in Zhongliangshan mine, Chongqing, southwestern China. The methods applied in this study are X-ray fluorescence spectrometry (XRF), inductively coupled mass spectrometry (ICP-MS), X-ray diffraction analysis (XRD) plus Siroquant, and scanning electron microscopy in conjunction with an energy-dispersive X-ray spectrometry (SEM-EDX). The results indicate that some trace elements including Li, Be, Sc, V, Cr, Co, Ni, Cu, Zn, Ga, Zr, Nb, Cd, Sb, REE, Hf, Ta, Re, Th, and U are enriched in the tuff from Zhongliangshan mine. The minerals in the tuff mainly include kaolinite, illite, pyrite, anatase, calcite, gypsum, quartz, and traces of minerals such as zircon, florencite, jarosite, and barite. The tuff is of mafic volcanic origin with features of alkali basalt. Some minerals including florencite, gypsum, barite and a portion of anatase and zircon have been derived from hydrothermal solutions. It is suggested that Zhongliangshan tuff is a potential polymetallic ore and the recovery of these valuable elements needs to be further investigated.

Keywords: geochemistry; mineralogy; origin; tuff; Chongqing

1. Introduction

With the depletion of traditional rare metal deposits, coal deposits as promising alternative sources for rare metals have attracted much attention in recent years [1–9]. At present, germanium is the most successful rare metal element that has been extracted from coal ash [4,8,9]. The three well-known coal-bearing strata hosted Ge deposits include Lincang (Yunnan Province) and Wulantuga (Inner Mongolia) of China, and Spetzugli of Russia, are the main sources for the industrial Ge at present and for the foreseeable future [1,4,8,9]. The super-large coal-bearing strata hosted gallium deposit in the Jungar Coalfield (Inner Mongolia), China, is another typical example discovered in 2006 [10], which was considered as the third and the most outstanding discovery after the coal-bearing strata hosted uranium and germanium deposits [2,10]. Moreover, aluminum is also enriched in Jungar coalfield [1,10]. In 2010, another new type of coal-bearing strata hosted Nb (Ta)-Zr (Hf)-REE-Ga polymetallic deposit of volcanic origin was discovered in the late Permian coal-bearing strata of eastern Yunnan, southwestern China [11]. Similar polymetallic deposits have since been discovered in some coalfields from southern China [1,3]. Similar to most typical areas enriched in rare metals in coal-bearing strata, the tectonic controls on the localization of the metalliferous coal deposits and the mechanisms of rare-metal mineralization in south China and south Primorye of Russia have been studied comparatively in detail [3]. The possible recovery of rare earth elements from coal and its combustion products such as fly ash is an exciting new research area [2,12–16], because coal and its combustion derivation (fly ash) may have elevated concentrations of these rare metals.

The purpose of this paper is to discuss the mineralogical and geochemical compositions of tuff layer in late Permian coal-bearing strata of Zhongliangshan mine, Chongqing, southwestern China. It also contributes to the discussion on the origin and potential prospects of rare metals mineralization of the tuff.

2. Geological Setting

The Zhongliangshan mine is located in the urban area of Chongqing, southwestern China (Figure 1). The coal-bearing sequence is the late Permian Longtan Formation (P_3l), which is composed of the light gray, gray, dark gray mudstone, sandy mudstone, siltstone, sandstone and coal seams. This formation is enriched in brachiopods, fern, cephalopods, bivalves, trilobite and other fossils. The Longtan Formation was deposited in a continental–marine transitional environment and has a thickness varying from 26.5 to 105.02 m, with an average of 71.08 m. It contains 10 coal seams, which are identified as K1 to K10 from top to bottom. The Changxin Formation conformably overlies the Longtan Formation and is mainly composed of thick layers of brown-gray, dark gray limestone intercalated with thin layers of mudstone and flint nodules. Some fossils including brachiopods, spindle dragonflies, sponges, corals, and trilobites are enriched in the Changxin Formation. The Maokou Formation disconformably underlies the Longtan Formation, which consists of thick layers of light gray to dark gray bioclastic limestone.

The tuff layer, with a thickness mostly of 2–5 m, light-gray or light-gray–white in color, and a conchoidal fracture and a soapy feel, is located at the lowermost Longtan Formation. The K10 coal seam conformably overlies the tuff layer, which has a disconformable contact with the underlying Maokou Formation (middle Permian) (Figure 2). The tuff is enriched in pyrite and shows massive bedding structure. The tuff was derived from the basalt eruption and deposited directly on the weathered surface of the Maokou Formation limestone, and then was subjected to weathering, leaching, and eluviation [17,18]. It is usually described as bauxite or bauxitic mudstone during core sample identification or field lithological description [17,18].

3. Samples and Analytical Procedures

A total of 21 bench samples were taken from the tuff layer in the Zhongliangshan mine, following the Chinese Standard GB/T 482-2008 [19]. Each tuff bench sample was cut over an area 10-cm wide, 10-cm deep and 10-cm thick. All collected samples were immediately stored in plastic bags to minimize contamination and oxidation. Large chips were selected at random from each sample for preparation of polished sections and also kept for later reference if required. The remainder of each sample was crushed and ground to pass through the 200-mesh sieve for analysis.

The loss of ignition (LOI) of each sample was determined according to ASTM standard D3174 [20]. All samples were analyzed by X-ray diffraction (XRD) using a D8 advance powder diffractmeter with Ni-filtered Cu-Kα radiation and a scintillation detector. The XRD pattern was recorded over a 2θ interval of 2.6°–70°, with a step size of 0.02°. X-ray diffractograms of the tuff samples were subjected to quantitative mineralogical analysis using Siroquant™ of China University of Mining and Technology (Beijing), a commercial interpretation software developed by Taylor [21] based on the principles for diffractogram profiling set out by Rietveld [22]. Further details indicating the use of this technique for coal-related materials are given by Ward *et al.* [23,24] and Ruan and Ward [25]. A Scanning Electron Microscope in conjunction with an energy-dispersive X-ray spectrometer (SEM-EDX, JEOL JSM-6610LV+OXFORD X-max, Tokyo, Japan), with an accelerating voltage of 20 kV, was used to study morphology and microstructure of minerals, and also to determine the distribution of some elements in tuff samples under a high vacuum mode in Chongqing Institute of Geology and Mineral Resources.

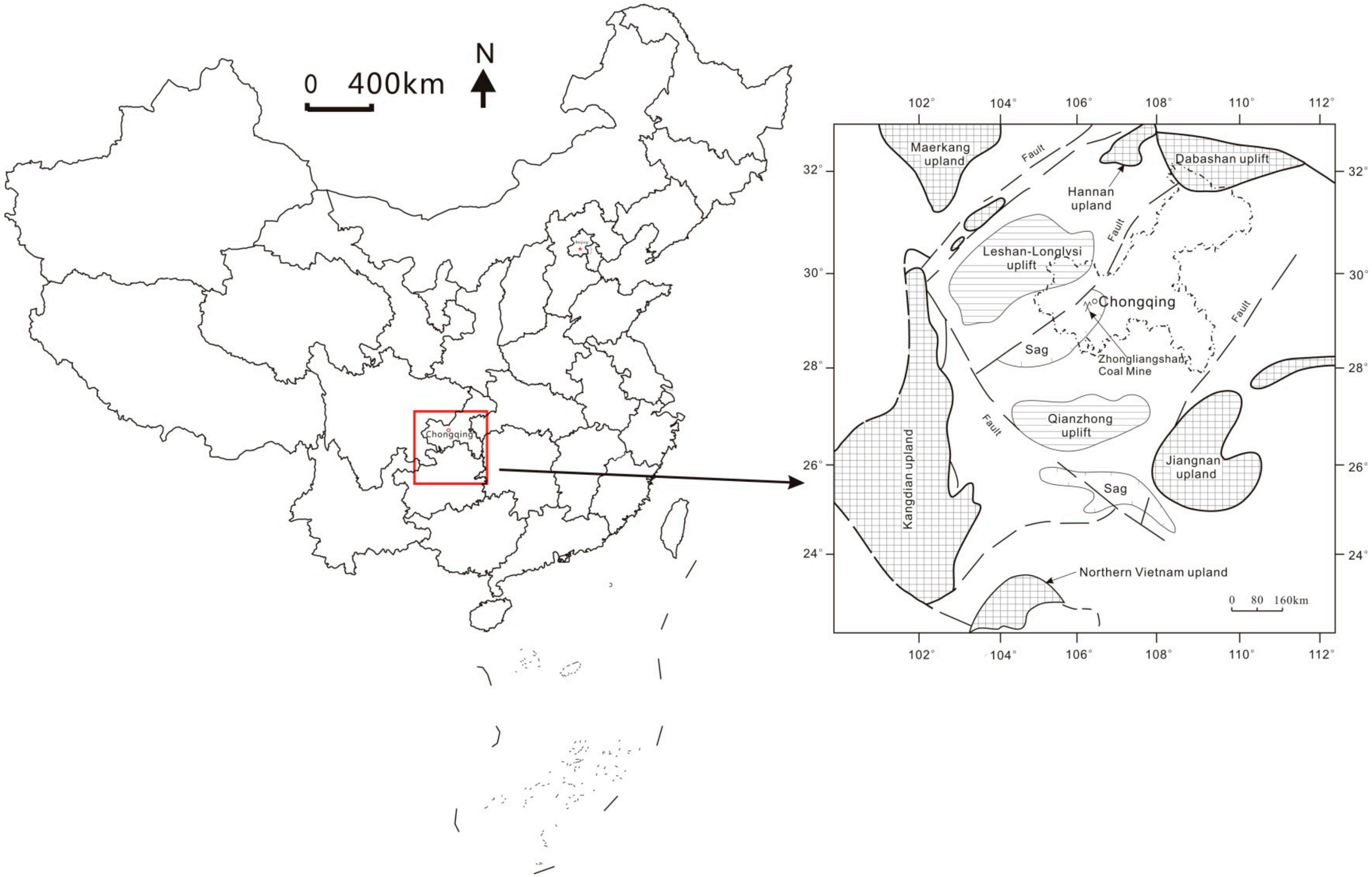

Figure 1. Location of the Zhongliangshan Mine, Chongqing, southwestern China.

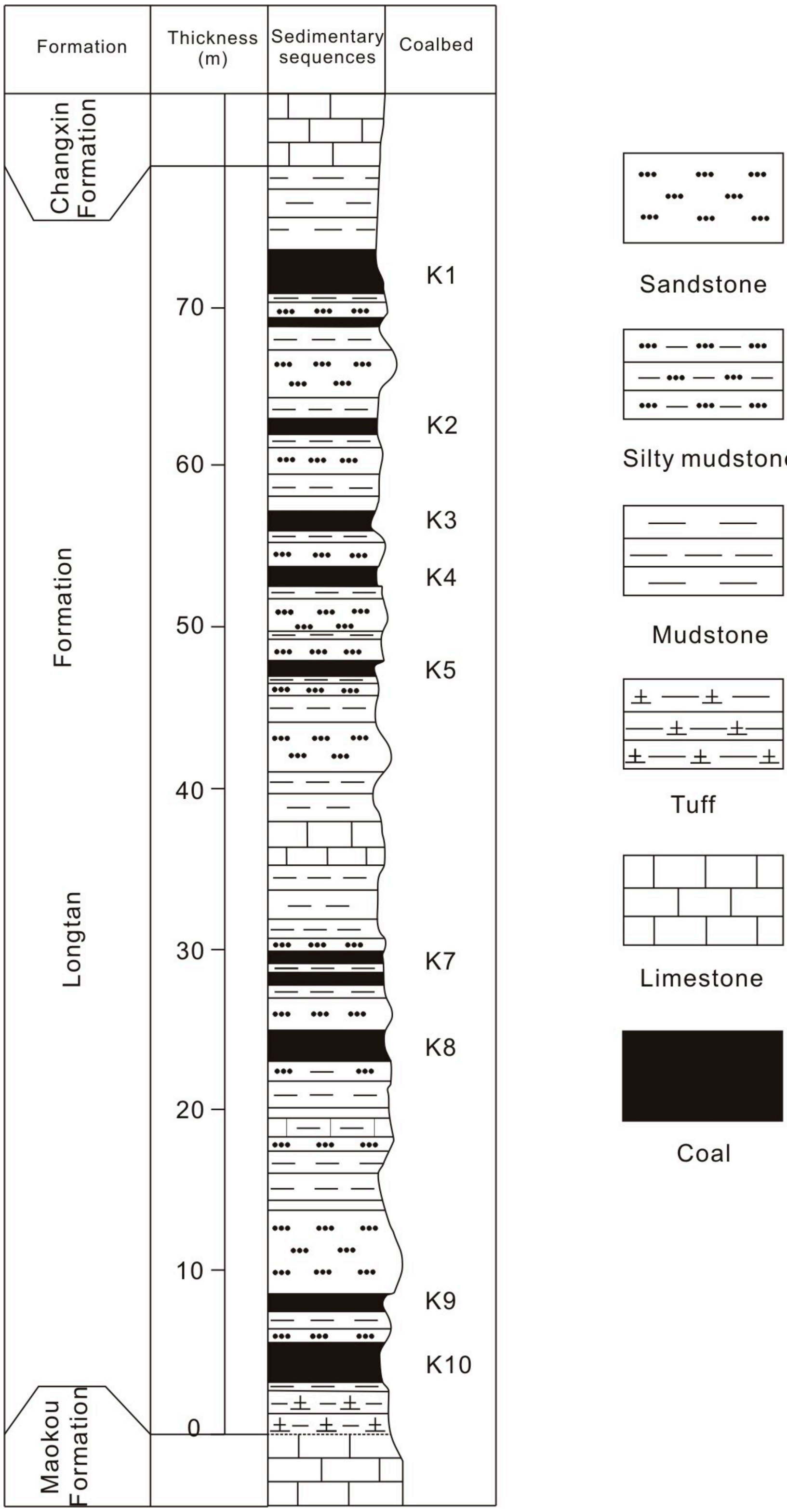

Figure 2. Generalized sedimentary sequence at the Zhongliangshan Mine, Chongqing.

Percentages of major element oxides including SiO_2, TiO_2, Al_2O_3, Fe_2O_3, MnO, MgO, CaO, Na_2O, K_2O, and P_2O_5 in the tuff samples were determined by X-ray fluorescence spectrometry (XRF) in Chongqing Institute of Geology and Mineral Resources. The contents of trace elements were determined by inductively coupled mass spectrometry (Thermo X series II ICP-MS, Thermo

Fisher Scientific, Waltham, MA, USA) in Chongqing Institute of Geology and Mineral Resources. The procedures of ICP-MS were: weigh 0.25 g sample in a 50 mL Teflon beaker; add 20 mL HNO_3-$HClO_4$-HF (volume ratio of 4:1:5) and 2 mL H_2SO_4; place on a temperature controlled heating plate and heat to 230 °C until like wet salt; then heat to 280 °C and evaporate to dryness; turn off the heating plate to cool the sample for 3 min; add 8 mL concentrated aqua regia; incubate for 10 min; transfer the solution to a 25 mL plastic flask; mix and volume; take 5 mL of solution to a 25 mL volumetric flask and dilute to the mark; and study using high resolution inductively coupled plasma mass spectrometry.

4. Results

4.1. Minerals

The proportion of each crystalline phase of the tuff identified by X-ray diffractometry plus Siroquant is given in Table 1. The minerals in Zhongliangshan tuff mainly include kaolinite, illite, pyrite, anatase, calcite, gypsum, and quartz. Some trace minerals such as zircon, florencite, jarosite, and barite, are observed under SEM-EDX.

Table 1. Mineral compositions of Tuff by XRD analysis and Siroquant (%).

Sample	Kaolinite	Illite	Pyrite	Anatase	Calcite	Quartz	Gypsum
S140SE7-1	83.2	-	13.6	2.7	-	0.5	-
S140SE7-2	85.1	-	9.3	3.5	-	2.1	-
S140SE7-3	65.4	-	11.6	8.2	-	14.8	-
S140SE7-4	69.9	-	20.2	6.7	-	3.3	-
S140SE7-5	53.7	-	38.2	2.8	-	-	5.3
S140SE7-6	61.4	-	30.8	3.2	-	-	4.6
S140SE7-7	61.9	-	19.8	4.1	-	-	14.2
S140SE7-8	78.7	-	14.8	3.3	-	0.1	3.1
S140SE7-9	80	-	10.6	7.5	-	0.3	1.7
S140SE7-10	65.8	-	26.5	4.7	-	0.3	2.7
S140SE7-11	72.4	-	16.1	8.8	-	0.3	2.5
S140SE7-12	73.4	6.7	2.8	14.3	-	0.4	2.4
S140SE7-13	49.9	18.6	10.6	9.7	6.1	0.3	4.8
S140SE7-14	11.4	3.8	28.8	0.8	45	-	10.3
S140SE7-15	52.9	21	3.1	8.4	10.7	0.5	3.5
S140SE7-16	81.5	4.4	1.4	6.9	3.8	0.1	1.8
S140SE7-17	86.4	4.4	1.1	6.9	-	-	1.2
S140SE7-18	80.7	6	2.4	7.2	0.4	0.4	2.8
S140SE7-19	34.5	31.3	1.9	3.6	24.7	0.3	3.7
S140SE7-20	67.2	18.6	1	10.5	0.1	0.5	2.2
S140SE7-21	56	35.3	0.4	7.2	0.3	-	0.7
Average	65.30	15.01	12.62	6.24	11.39	1.61	3.97

4.1.1. Kaolinite and Illite

Kaolinite is the dominant mineral of the tuff in Zhongliangshan (Figure 3). The average content of kaolinite is up to 65.3%, and all the samples are richer than 50% except for samples S140SE7-13, S140SE7-14, and S140SE7-19. Kaolinite occurs mainly as matrix material (Figure 4A), and to a lesser extent, as vermicular (Figure 4B) and individual massive (Figure 4C). Illite occurs at the lower part of the profile (Figure 3).

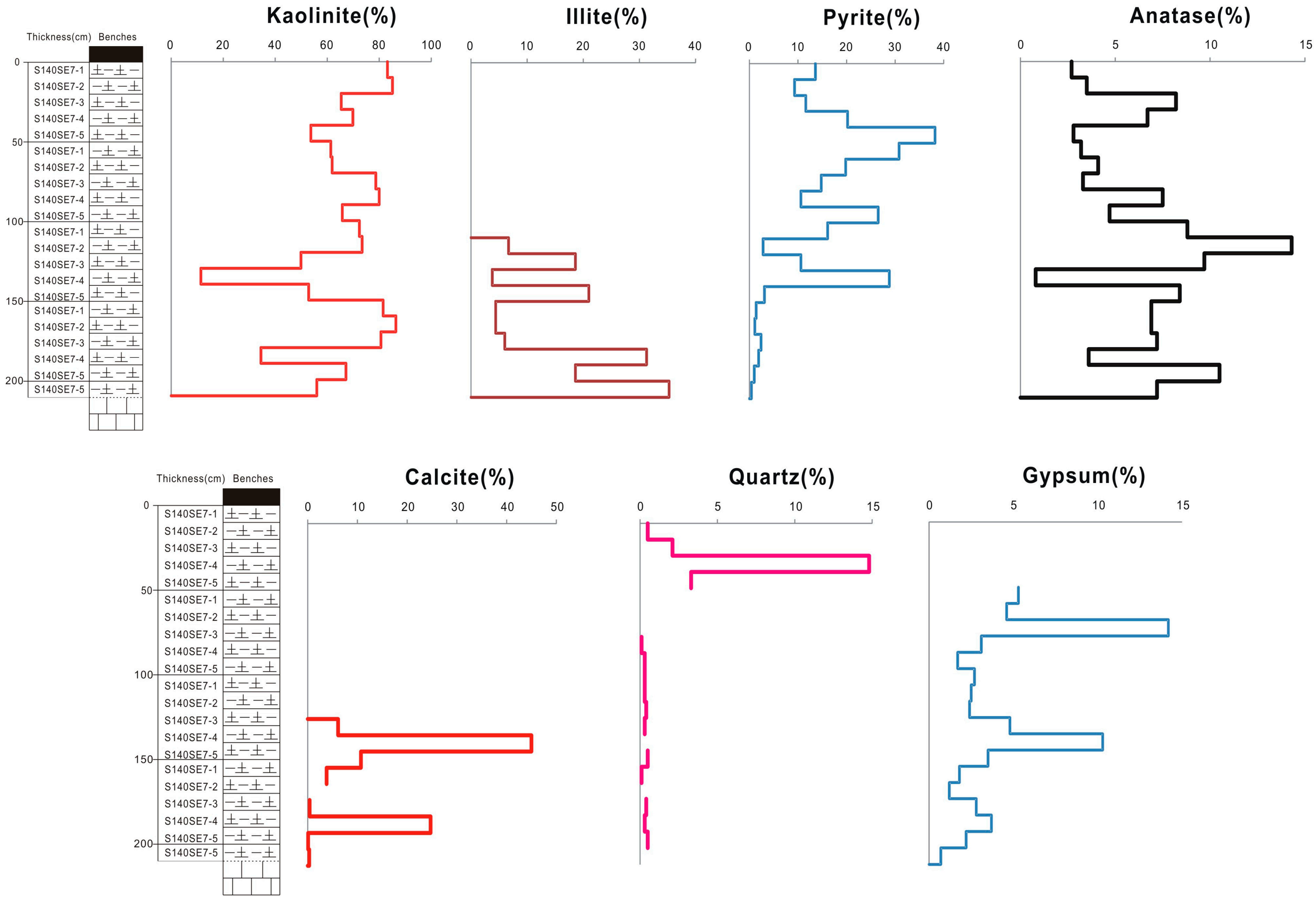

Figure 3. Vertical variations of minerals from the tuff in the Zhongliangshan mine.

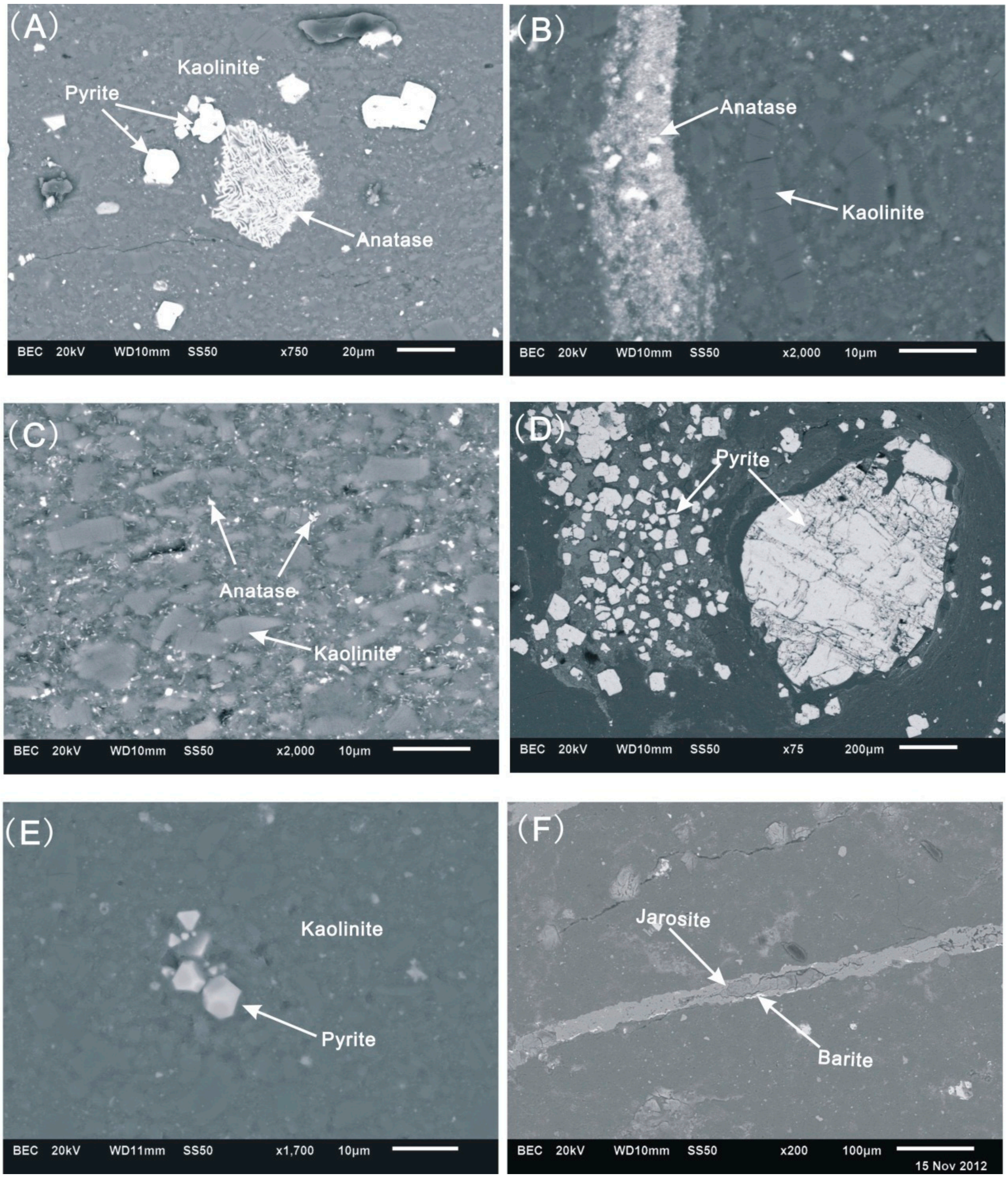

Figure 4. Back scattered images of minerals in the Zhongliangshan tuff: (**A**) kaolinite, pyrite and anatase in sample S140SE7-1; (**B**) kaolinite and anatase in sample S140SE7-8; (**C**) kaolinite and anatase in sample S140SE7-1; (**D**) pyrite in sample S140SE7-4; (**E**) pyrite and kaolinite in sample S140SE7-6; and (**F**) jarosite and barite in sample S140SE7-18.

4.1.2. Pyrite, Jarosite and Barite

Pyrite distributes widely in the tuff samples and its content varies from 0.4% to 38.2% (12.6% on average). Its content is gradually decreasing from top to bottom (Figure 3), suggesting that the upper portion has been more subjected to seawater. Pyrite mainly occurs as discrete particles (Figure 4A,D), lumps (Figure 4D), and in some cases, as cubic crystal and pentagonal dodecahedron (Figure 4E). Jarosite occurs as fracture-fillings (Figure 4F), indicating a weathering product of pyrite. Barite is located on the edge of jarosite (Figure 4F), which may be formed by the reaction of jarosite with the hydrothermal solution containing Ba.

4.1.3. Anatase

Anatase is present evenly in the tuff samples and varies from 0.8% to 14.3% with an average of 6.2%. The content of Nb in the anatase is up to 0.18% determined by SEM-EDX. Anatase occurs mainly as irregular fine particles (Figure 4B,C) or as colloidal (Figures 4A and 5A) in the kaolinite matrix.

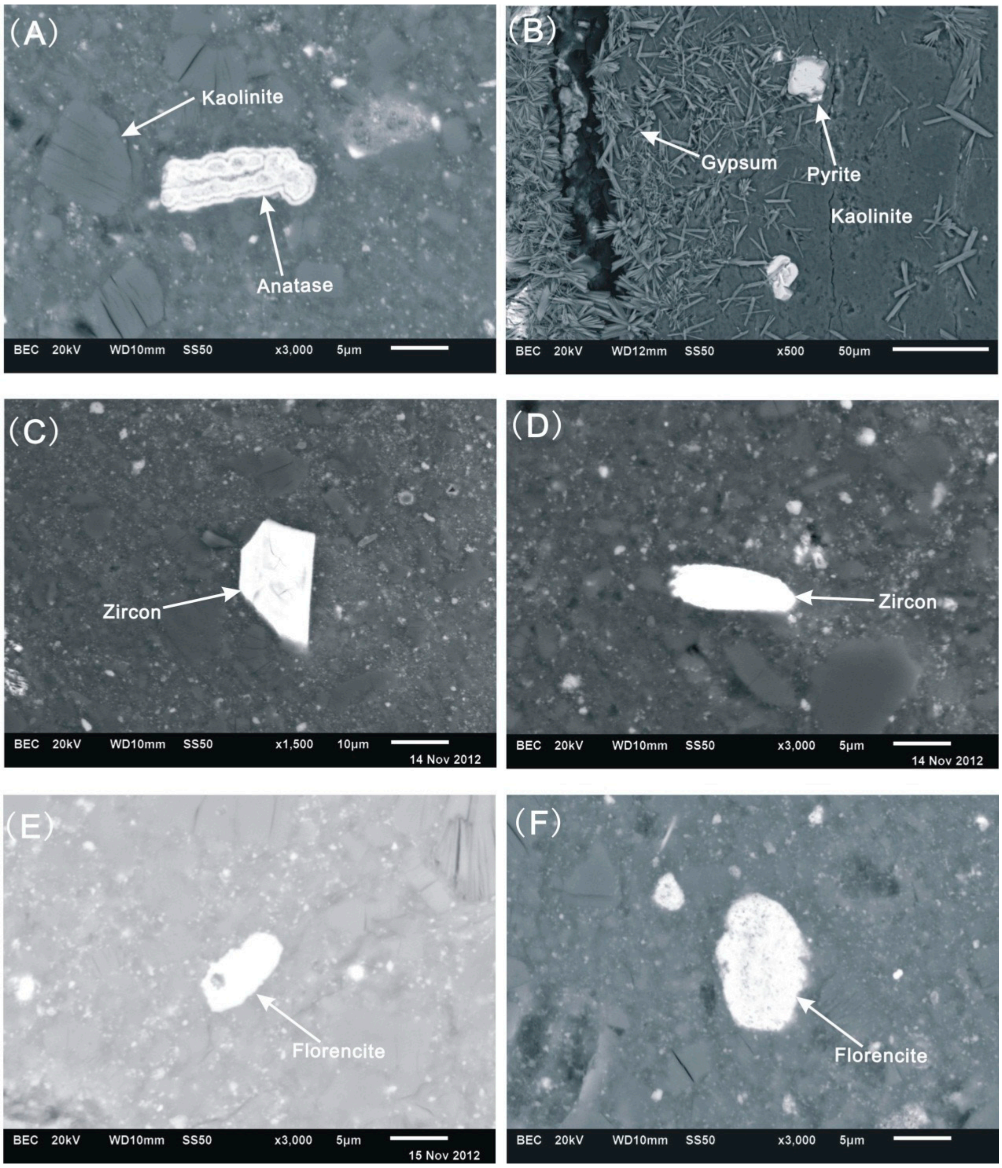

Figure 5. Back scattered images of minerals in the Zhongliangshan tuff: (**A**) kaolinite and anatase in sample S140SE7-4; (**B**) gypsum, pyrite, and kaolinite in sample S140SE7-10; (**C**) zircon in sample S140SE7-15; (**D**) zircon in the sample S140SE7-15; (**E**) florencite in sample S140SE7-21; and (**F**) florencite in sample S140SE7-4.

4.1.4. Calcite and Gypsum

Calcite distributes at the lower portion of the profile (Table 1, Figure 3), similar to that of illite. Gypsum occurs as radiating forms in the tuff and is present on the edge of fractures (Figure 5B), indicating an epigenetic origin.

4.1.5. Zircon and Florencite

Although zircon and florencite are at concentration below the detection limit of the XRD and Siroquant analysis, they have been observed under SEM-EDX in the tuff samples of the present study. Zircon occurs as subhedral (Figure 5C) and long axis (Figure 5D) in the kaolinite matrix. Florencite occurs as ellipsoidal form in kaolinite; however, minerals containing medium (M-REE) and heavy-rare earth elements (H-REE) have not been observed (M-REE include Eu, Gd, Tb, Dy, and Y; and H-REE include Ho, Er, Tm, Yb, and Lu [7]).

4.2. Major Elements

The loss of ignition of the tuff samples varies from 13.94% to 23.56%, with an average of 17.7%. The major element oxides are mainly represented by SiO_2 (35.3% on average) and Al_2O_3 (29.23%), followed by Fe_2O_3 (10.95%) and TiO_2 (3.82%) (Table 2). The ratio of SiO_2/Al_2O_3 is from 1.16 to 1.26 and averages 1.21, higher than the theoretical value of kaolinite (1.18). The ratio of TiO_2/Al_2O_3 is from 0.09 to 0.15, with an average of 0.13.

4.3. Trace Elements

Compared with the average concentration of the Upper Continental Crust (UCC) [26], some trace elements are enriched in the tuff samples from Zhongliangshan mine (Table 2). The concentration coefficients (CC, the ratio of the trace-element concentrations in investigated samples *vs.* UCC) of trace elements higher than 10 include Li, Cr, Cu, Cd, Sb and Re; whereas the elements with CC between 5 and 10 include V, Ni, Zr, Hf, and U. Elements Be, Sc, Co, Zn, Ga, Nb, REE, Ta, and Th, have a CC between 2 and 5. Elements Rb, Sr, Ba, and Tl are depleted, with a CC < 0.5. Other trace elements have concentrations close to the UCC, with CC between 0.5 and 2.

4.3.1. Scandium

The average content of Sc in tuff samples is 30.1 μg/g, which is close to these of the tuffs from Songzao (29.8 μg/g), Nanchuan (26.3 μg/g) and the mafic rocks (29 μg/g, 1060 samples) [27]. Scandium is immobile during weathering and alteration and thus can be used as a reliable indicator for the source of tonsteins in coal-bearing strata system [28,29].

4.3.2. Vanadium, Cr, Co and Ni

The average contents of V, Cr, Co and Ni in the investigated samples are 576, 360, 39.8, and 114 μg/g, respectively, close to the tuff from Songzao (V, Cr, Co, and Ni being 576, 549, 37.9, and 164 μg/g, respectively) [1,3] and the normal detrital sediments (888 samples) in the south of Sichuan Province surrounding Chongqing (V, Cr, Co, and Ni being 442, 206, 31, and 61 μg/g, respectively) [30]. The contents of V and Cr have the same variations through the seam section, gradually increasing from top to bottom (Figure 6). However, the contents of Co and Ni are higher in the middle relative to the upper and lower portions (Figure 6). The terrigenous source of the inorganic matter in the late Permian coals and normal sediments in southwestern China is the Emeishan Basalt of the Kangdian Upland, which is enriched in V, Cr, Co, and Ni [31,32]. The values of tuff samples in the Zhongliangshan mine are close to those in normal sediments, indicating the normal sediments in southwestern China and tuff in Zhongliangshan have the same magmatic sources (the Emeishan basalt magma enriched in V, Cr, Co, and Ni). Dai *et al.* [1,3,18] suggested that some dark minerals such as basic plagioclase and pyroxene in the basalt rocks could be easily decomposed under weathering conditions and then transported into coal-bearing basin as complex anions.

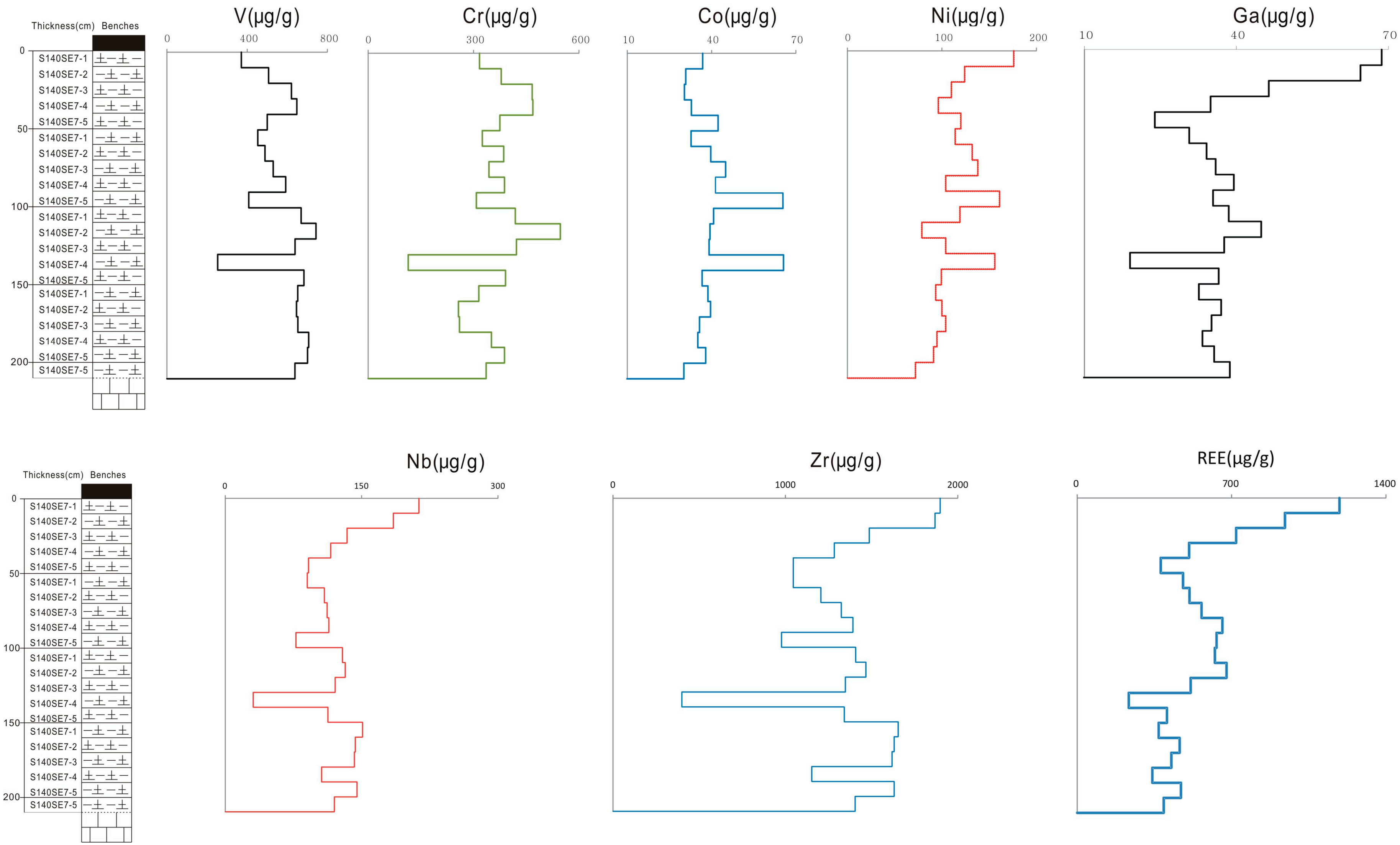

Figure 6. Vertical variations of selected trace elements of the tuff in Zhongliangshan mine, Chongqing.

Table 2. Elemental concentrations in Tuff samples from the Zhongliangshan Mine (elements in μg/g, Oxides in %).

Sample	LOI	SiO_2	TiO_2	Al_2O_3	Fe_2O_3	MnO	MgO	CaO	Na_2O	K_2O	P_2O_5	FeO	SiO_2/Al_2O_3	TiO_2/Al_2O_3	Li	Be	Sc	V	Cr	Co	Ni	Cu
S140SE7-1	19.87	36.25	2.77	31.23	9.1	0.012	0.26	0.12	0.14	0.1	0.075	0.6	1.16	0.09	454	9.46	33.4	371	317	36.8	176	247
S140SE7-2	17.87	38.9	3.21	33.6	5.52	0.009	0.26	0.1	0.31	0.1	0.04	0.55	1.16	0.1	445	9.91	38	507	379	30.8	124	243
S140SE7-3	18.15	36.84	3.82	30.98	9.52	0.02	0.2	0.11	0.22	0.1	0.051	0.5	1.19	0.12	349	7.55	31.8	621	467	30.3	110	245
S140SE7-4	19.66	32.69	3.63	27.44	15.46	0.21	0.19	0.14	0.17	0.1	0.051	0.8	1.19	0.13	367	6.33	29.1	648	469	32.8	96.2	259
S140SE7-5	23.56	24.78	2.57	20.01	28.09	0.015	0.18	0.36	0.13	0.085	0.037	0.75	1.24	0.13	337	5.66	25.6	500	375	42.3	120	258
S140SE7-6	21.65	28.05	2.92	23.17	23	0.015	0.22	0.31	0.15	0.094	0.046	0.6	1.21	0.13	299	5.42	24	453	325	32.7	114	235
S140SE7-7	19.52	32.7	3.28	27.62	16.08	0.012	0.27	0.12	0.15	0.11	0.043	0.4	1.18	0.12	421	6.95	28.2	489	386	39.7	132	286
S140SE7-8	19.06	33.86	3.35	28.75	14.17	0.013	0.31	0.12	0.17	0.13	0.048	0.4	1.18	0.12	401	6.61	32.4	530	344	45	138	278
S140SE7-9	16.45	38.23	3.87	32.89	7.81	0.008	0.25	0.11	0.16	0.11	0.049	0.35	1.16	0.12	442	7.11	33.3	592	388	41.4	104	251
S140SE7-10	20.62	29.97	2.89	24.88	20.9	0.011	0.23	0.17	0.11	0.13	0.03	0.55	1.2	0.12	311	4.87	24.7	408	308	65.4	161	282
S140SE7-11	17.82	35.72	4.38	29.64	11.54	0.004	0.15	0.26	0.21	0.17	0.066	0.5	1.21	0.15	321	7.34	33.2	669	419	40.7	119	316
S140SE7-12	15.42	40.12	4.65	33.07	5.18	0.007	0.2	0.26	0.49	0.43	0.086	0.25	1.21	0.14	248	7.59	36.5	743	547	39.4	78.8	330
S140SE7-13	17.93	35.93	4.39	29.44	9.57	0.008	0.2	1.56	0.3	0.43	0.067	0.6	1.22	0.15	219	6.48	30.7	639	422	39.1	104	266
S140SE7-14	18.09	15.54	1.55	11.23	31.32	0.039	0.43	20.38	0.16	0.65	0.017	1.75	1.38	0.14	31.5	2.16	12.6	253	114	65.6	156	146
S140SE7-15	15.61	38.45	4.33	30.94	5.28	0.01	0.33	3.4	0.53	0.82	0.05	0.85	1.24	0.14	170	6.3	31.3	683	391	36.6	99.4	188
S140SE7-16	14.89	40.64	5.28	34.4	1.94	0.006	0.16	1.52	0.5	0.25	0.045	0.4	1.18	0.15	254	7.2	35.7	652	315	38.7	93.4	265
S140SE7-17	14.91	41.58	5.03	35.15	1.99	0.004	0.21	0.13	0.49	0.37	0.056	0.35	1.18	0.14	299	6.89	34.8	646	257	39.6	100	255
S140SE7-18	15.35	40.55	4.89	34.01	3.47	0.004	0.24	0.4	0.49	0.49	0.059	0.85	1.19	0.14	258	6.31	33.1	653	260	35.7	104	265
S140SE7-19	15.5	37.44	4.08	29.19	4.03	0.013	0.59	6.57	0.72	1.47	0.045	0.9	1.28	0.14	153	5.66	25	707	351	35.1	94.7	199
S140SE7-20	13.94	42.07	5.01	34.88	1.83	0.003	0.32	0.47	0.47	0.76	0.06	0.55	1.21	0.14	246	6.79	32.1	701	388	37.9	91.2	281
S140SE7-21	15.82	40.92	4.24	32.45	3.12	0.004	0.46	1.12	0.53	1.26	0.055	1.3	1.26	0.13	168	5.58	26.8	638	336	30.1	72	193
Average	17.7	35.3	3.82	29.28	10.9	0.02	0.27	1.8	0.31	0.39	0.05	0.66	1.21	0.13	295	6.58	30.1	576	360	39.8	114	252
UCC	nd	nd	nd	nd	nd	nd	nd	nd	nd	nd	nd	nd	nd	nd	20	3	11	60	35	10	20	25
CC	nd	nd	nd	nd	nd	nd	nd	nd	nd	nd	nd	nd	nd	nd	14.7	2.2	2.7	9.6	10.3	4	5.7	10.1

Sample	Zn	Ga	Rb	Sr	Zr	Nb	Mo	Cd	In	Sb	Cs	Ba	Hf	Ta	W	Re	Tl	Pb	Bi	Th	U
S140SE7-1	237	68.7	3.98	292	1898	213	3.4	3.13	0.615	4.22	1.17	146	57.6	15.9	4.02	0.042	0.11	58.1	1.41	50.3	25.7
S140SE7-2	190	64.5	2.86	190	1868	185	2.12	2.04	0.654	2.82	1.15	113	51.4	14.6	3.52	0.02	0.058	40.4	1.21	49.7	24.5
S140SE7-3	143	46.4	2.96	282	1487	134	1.73	0.952	0.587	3.51	1.48	141	37.7	8.88	4.44	0.018	0.085	39	1.62	33.4	9.83
S140SE7-4	123	34.9	3.52	256	1284	116	1.8	1.7	0.719	3.7	1.4	122	33.4	8.29	3.44	0.013	0.087	47.4	1.63	28.2	9.71
S140SE7-5	107	23.9	3.2	166	1046	91.6	1.56	1.46	0.457	4.13	1.07	92	26	6.91	3.16	0.014	0.207	61.3	1.22	23.8	8.11
S140SE7-6	100	30.7	2.03	191	1046	90.2	1.22	1.31	0.437	4.23	0.892	89.6	27.1	5.96	2.75	0.007	0.24	53.5	1.15	23.4	8.97
S140SE7-7	109	34.1	3.69	188	1206	109	0.985	1.22	0.494	3.41	1.1	101	30.7	7.6	2.83	0.006	0.103	49.3	1.35	27.9	11.4
S140SE7-8	124	35.9	3.1	232	1324	112	1.04	1.31	0.541	3.91	1.1	115	33.8	7.82	3.66	0.009	0.189	55.2	1.51	29	13.2
S140SE7-9	115	39.5	2.66	194	1392	114	1.03	1.5	0.519	2.23	1.05	99.3	36.9	8.57	3.67	0.006	0.058	34	1.48	30.4	16.6
S140SE7-10	103	35.4	2.46	154	978	77.7	1.45	1.83	0.516	6.79	0.927	79.1	25.4	5.68	2.8	0.01	0.09	75.2	1.14	21.7	12.6
S140SE7-11	192	38.5	5.34	287	1408	129	1.54	2.77	0.6	2.73	1.94	127	36.1	8.79	3.88	0.006	0.093	44	1.73	30	16
S140SE7-12	178	44.9	14.9	325	1467	132	1.68	4.45	0.572	1.71	5.03	141	37.9	8.98	4.05	0.013	0.118	23.6	2.06	31.8	17.7
S140SE7-13	161	37.6	12.5	341	1348	121	1.67	5.14	0.627	2.21	3.52	137	33.2	8.27	3.41	0.006	0.134	33.8	1.69	28.5	14
S140SE7-14	108	19	14.9	503	400	30.7	0.712	18.4	0.211	3.32	1.66	60.3	9.45	2.28	1.7	0.008	0.292	34.9	0.595	8.57	5.46
S140SE7-15	148	36.5	23.7	404	1342	113	1.37	6.96	0.501	2.08	5.27	143	34.9	7.88	3.69	0.006	0.156	26.9	1.52	28.7	14.2
S140SE7-16	170	32.6	6.83	279	1654	151	1.78	3.52	0.628	1.27	1.96	131	41.3	10.4	4.61	0.018	0.071	19.6	1.34	34	17.4
S140SE7-17	166	37	9.09	261	1631	143	0.996	4	0.567	1.68	2.37	131	41.4	10.1	3.76	0.025	0.08	23.8	1.36	32.2	18.5
S140SE7-18	147	35.1	12.1	286	1619	142	1.4	3.55	0.531	1.99	2.25	137	39.8	9.76	3.74	0.013	0.08	26.1	1.39	32	19.5
S140SE7-19	139	33.3	39.5	387	1153	106	1.49	6.92	0.505	2.42	5.33	160	28.8	7.07	3.48	0.036	0.287	21.8	1.39	27	20.1
S140SE7-20	174	35.6	19.8	322	1631	145	1.6	4.14	0.578	1.76	3.18	158	41.4	9.92	4.05	0.009	0.164	23	1.55	34	26.4
S140SE7-21	153	38.7	31.1	323	1405	120	1.48	3.47	0.526	1.5	4.24	165	35	8.39	3.43	0.015	0.236	25.2	1.27	29	23.8
Average	147	38.2	10.5	279	1361	123	1.53	3.8	0.54	2.93	2.29	123	35.2	8.67	3.53	0.01	0.14	38.9	1.41	30.2	15.9
UCC	71	17	112	350	190	25	1.5	0.1	nd	0.2	3.7	550	5.8	2.2	2	0.0004	0.8	20	nd	10.7	2
CC	2.1	2.2	0.1	0.8	7.2	4.9	1	38	nd	14.7	0.6	0.2	6.1	3.9	1.8	35.7	0.2	1.9	nd	2.8	7.9

UCC, the Upper Continental Crust; CC, concentration coefficient of trace elements in the tuff, normalized by average trace element concentrations in UCC [26]; nd, no data.

4.3.3. Niobium, Ta, Zr and Hf

The average contents of Nb, Ta, Zr, and Hf of tuff in Zhongliangshan mine are 123, 8.67, 1361, and 35.2 μg/g, respectively, being close to those of the tuff from Songzao (Nb, Ta, Zr and Hf being 118, 9.46, 1377, and 41.5 μg/g, respectively). The Nb and Zr display a similar trend, both gradually decreasing from top to bottom (Figure 6).

The concentration of $(Nb, Ta)_2O_5$ of tuff in Zhongliangshan mine varies from 47 to 324 μg/g and averages 186 μg/g, lower than the concentration of the late Permian "Nb (Ta)-Zr (Hf)-Ga-REE" polymetallic deposit discovered in eastern Yunnan, southwestern China [11]. $(Zr, Hf)O_2$ varies from 551 to 2632 μg/g and averages 1880 μg/g, which does not meet the minimum industrial grade of the weathering crust type deposit (8000 μg/g) [33].

The common Nb-, Zr-, REE-, and Ga-bearing minerals have rarely been observed in the tuff, and thus it is suggested that these rare metals probably occur as absorbed ions [11,29]. However, Nb may occur as isomorph in the Ti-bearing minerals (Figure 4B,C) and Zr occurs as zircon (Figure 5C,D) in studied samples.

4.3.4. Gallium

The concentration of Ga in Zhongliangshan tuff varies from 19 to 68.7 μg/g and averages 38.2 μg/g, higher than the minimum industrial grade in bauxite (20 μg/g) and coal (30 μg/g) [34], but lower than the concentration of the late Permian "Nb(Ta)-Zr(Hf)-Ga-REE" polymetallic deposit in eastern Yunnan, southwestern China [11]. From top to bottom, the concentration of Ga gradually decreases, consistent with those of the Nb and Zr. Because the geochemical nature of Ga is similar to Al [1,8], it may occur as isomorph in Al-bearing minerals (e.g., kaolinite).

4.4. Rare Earth Elements (REE)

In this study, REE is used to specifically represent the elemental suite La, Ce, Pr, Nd, Sm, Eu, Gd, Tb, Dy, Y, Ho, Er, Tm, Yb, and Lu [35]. The abundances and geochemical parameters of REE in the tuff samples are listed in Tables 3 and 4 respectively. The concentration of REE varies from 234 to 1189 μg/g, with an average of 548 μg/g. The concentration of REE gradually decreases from top to bottom, similar to that of Nb and Zr. Yttrium is closely associated with lanthanides in nature, because its ionic radius is very similar and its ionic charge is equal to that of Ho [7]. For this reason, yttrium is generally placed between Dy and Ho in normalized REE patterns [36]. Based on Seredin-Dai's classification [7], a three-fold geochemical classification of REE was used in the present study, including light (L-REE: La, Ce, Pr, Nd, and Sm), medium (M-REE: Eu, Gd, Tb, Dy, and Y), and heavy (H-REE: Ho, Er, Tm, Yb, and Lu) REE [7]. Accordingly, three enrichment types are identified, L-type (light REE; $La_N/Lu_N > 1$), M-type (medium REE; $La_N/Sm_N < 1$, $Gd_N/Lu_N > 1$), and H-type (heavy REE: $La_N/Lu_N < 1$), in comparison with the upper continental crust [7]. This classification has been widely adopted and used in recent years [2].

Table 4 and Figure 7 illustrate that the tuff in the Zhongliangshan mine is mainly enriched in heavy REE. Only samples S140SE7-1, S140SE7-3, S140SE7-4, S140SE7-6, and S140SE7-8 are enriched in light REE; and samples S140SE7-2, S140SE7-10, and 140SE7-14 are enriched in medium REE. From top to bottom, the light REE enrichment only occurs in the upper portion of the profile, while the lower portion is enriched in heavy REE and the medium REE enrichment occasionally occurs in the middle portion.

The Ce-anomaly (expressed as δCe) values vary from 0.70 to 1.77, with an average of 1.41, indicating a well-pronounced Ce positive anomaly. The REE distribution patterns of the tuff display positive Ce anomalies, owing to the in-situ precipitation of Ce^{4+} in the process of weathering, leaching, and eluviation [35]. The Eu-anomaly (δEu) values varying from 0.76 to 1.51, with an average of 1.06, show a slight Eu positive anomaly, indicating the tuff and the Emeishan basalt have the same origin [35]. From top to bottom, δCe and δEu markedly increase. The distribution of REE of the tuff in the Zhongliangshan mine appears as a sawtooth shape, the portions of La-Sm and Gd-Lu occurring gentle and small slope, which indicates that the fractionation of REE is low.

Table 3. Rare earth elements in the tuff samples collected from the Zhongliangshan Mine (μg/g).

Sample	La	Ce	Pr	Nd	Sm	Eu	Gd	Tb	Dy	Y	Ho	Er	Tm	Yb	Lu
S140SE7-1	266	372	55.7	212	34.3	5.38	30	4.92	28.3	142	5.19	15.7	2.38	13.2	1.88
S140SE7-2	180	314	41.8	174	32.2	4.79	25.9	4.22	22.9	111	4.79	12	2.08	10.8	1.67
S140SE7-3	134	313	26.8	93.9	16.9	2.99	15.4	2.94	16.2	76.8	2.99	8.08	1.23	8.02	1.25
S140SE7-4	103	224	17.8	61.1	8.7	1.83	10.4	1.87	10.9	52.7	2.11	5.66	0.929	5.45	0.897
S140SE7-5	74.6	152	12.8	48.1	8.55	1.79	8.32	1.76	9.73	46.7	1.81	5.28	0.843	5.4	0.837
S140SE7-6	91.5	201	18.2	66.4	13.7	2.58	11.2	1.97	9.95	49.5	1.73	5.21	0.796	5.23	0.763
S140SE7-7	95.7	237	16.5	52.9	9.71	2.09	9.78	1.93	9.99	56.6	2.02	5.97	1.03	6.63	0.996
S140SE7-8	108	265	17.6	59.6	10.7	2.05	10.2	2.03	11.1	59.1	2.15	6.5	1.21	7.37	0.986
S140SE7-9	111	338	19.8	67.4	11.9	2.5	11.7	2.24	11.8	62.2	2.27	7.23	1.22	7.69	1.19
S140SE7-10	77.7	293	22.9	107	29	5.19	18.7	2.42	10.9	50	1.87	5.5	0.895	5.65	0.866
S140SE7-11	103	297	22.3	79.7	14.7	2.47	11.4	2.23	12.4	58.3	2.42	7.58	1.28	8.05	1.23
S140SE7-12	106	326	24.4	87.8	15.7	2.91	12.5	2.33	13.6	62.5	2.65	8.38	1.42	9.21	1.43
S140SE7-13	76.5	251	17.7	60.4	10.4	2.46	9.64	2.04	12	52.7	2.26	6.79	1.18	7.91	1.12
S140SE7-14	18.9	101	9.12	45.4	12.7	2.56	7.86	1.23	5.44	22.9	0.907	2.45	0.367	2.45	0.326
S140SE7-15	57.3	184	13	47.7	9	2.22	8.96	1.98	10.7	53.5	2.16	6.45	1.13	7.54	1.04
S140SE7-16	46.2	163	10.7	40.3	9.95	2.44	9.47	2.13	12.2	54.7	2.17	6.58	1.12	7.07	1.06
S140SE7-17	67.2	222	15.4	55.7	9.3	2.59	9.83	2.01	11.9	50.8	2.2	6.38	1.13	6.99	1.08
S140SE7-18	61.8	201	13.7	50.2	9.63	2.64	9.67	1.96	10.5	48.9	2.09	6	1.01	6.68	1.04
S140SE7-19	50.7	158	11.1	37.9	8.35	2.43	7.86	1.45	8.4	41.1	1.56	4.65	0.799	5.21	0.714
S140SE7-20	67.3	241	14.3	49.6	10.3	3.03	10.7	1.73	10.1	46.8	1.86	5.59	0.939	6.37	0.913
S140SE7-21	56.1	197	12.2	43.3	8.68	2.79	8.27	1.46	8.61	40	1.67	4.98	0.817	5.35	0.827
Average	93.0	240	19.7	73.4	14.0	2.84	12.3	2.23	12.3	58.99	2.33	6.81	1.13	7.06	1.05

Table 4. Rare earth elements geochemical parameters of Zhongliangshan tuff.

Sample	REE (μg/g)	LREE (μg/g)	MREE (μg/g)	HREE (μg/g)	L/M	L/H	M/H	$(La/Lu)_N$	$(La/Sm)_N$	$(Gd/Lu)_N$	δCe	δEu
S140SE7-1	1189	940	211	38.4	4.46	24.51	5.49	1.41	1.16	1.26	0.70	0.77
S140SE7-2	942	742	169	31.3	4.40	23.68	5.39	1.08	0.84	1.22	0.83	0.76
S140SE7-3	721	585	114	21.6	5.11	27.10	5.30	1.07	1.19	0.97	1.19	0.85
S140SE7-4	507	415	77.7	15.0	5.34	27.56	5.16	1.15	1.78	0.92	1.19	0.88
S140SE7-5	379	296	68.3	14.2	4.33	20.89	4.82	0.89	1.31	0.78	1.12	0.98
S140SE7-6	480	391	75.2	13.7	5.20	28.47	5.48	1.20	1.00	1.16	1.12	0.96
S140SE7-7	509	412	80.4	16.6	5.12	24.74	4.83	0.96	1.48	0.78	1.36	0.99
S140SE7-8	564	461	84.5	18.2	5.46	25.30	4.64	1.10	1.51	0.82	1.39	0.90
S140SE7-9	658	548	90.4	19.6	6.06	27.96	4.61	0.93	1.40	0.78	1.64	0.97
S140SE7-10	632	530	87.2	14.8	6.07	35.83	5.90	0.90	0.40	1.70	1.58	1.02
S140SE7-11	624	517	86.8	20.6	5.95	25.13	4.22	0.84	1.05	0.73	1.41	0.88
S140SE7-12	677	560	93.8	23.1	5.97	24.25	4.06	0.74	1.01	0.69	1.46	0.95
S140SE7-13	514	416	78.8	19.3	5.28	21.60	4.09	0.68	1.10	0.68	1.56	1.13
S140SE7-14	234	187	40.0	6.5	4.68	28.79	6.15	0.58	0.22	1.90	1.75	1.18
S140SE7-15	407	311	77.4	18.3	4.02	16.98	4.22	0.55	0.96	0.68	1.54	1.14
S140SE7-16	369	270	80.9	18.0	3.34	15.01	4.50	0.44	0.70	0.71	1.67	1.15
S140SE7-17	465	370	77.1	17.8	4.79	20.79	4.34	0.62	1.08	0.72	1.57	1.24
S140SE7-18	427	336	73.7	16.8	4.57	20.00	4.38	0.59	0.96	0.73	1.58	1.26
S140SE7-19	340	266	61.2	12.9	4.34	20.57	4.74	0.71	0.91	0.87	1.52	1.38
S140SE7-20	471	383	72.4	15.7	5.29	24.41	4.62	0.74	0.98	0.93	1.77	1.33
S140SE7-21	392	317	61.1	13.6	5.19	23.25	4.48	0.68	0.97	0.79	1.72	1.51
Average	548	441	88.6	18.4	5.00	24.13	4.83	0.85	1.05	0.94	1.41	1.06

ΣREE, sum of La, Ce, Pr, Nd, Sm, Eu, Gd, Tb, Dy, Y, Ho, Er, Tm, Yb, and Lu; LREE, sum of La, Ce, Pr, Nd, and Sm; MREE, sum of Eu, Gd, Tb, Dy and Y; HREE, sum of Ho, Er, Tm, Yb, and Lu; L/M, ratio of LREE and MREE; L/H, ratio of LREE and HREE; M/H, ratio of MREE and HREE; $(La/Lu)_N$, ratio of $(La)_N$ and $(Lu)_N$; $(La/Sm)_N$, ratio of $(La)_N$ and $(Sm)_N$; $(Gd/Lu)_N$, ratio of $(Gd)_N$ and $(Lu)_N$; $\delta Ce = Ce_N/(La_N \times Pr_N)^{1/2}$; $\delta Eu = Eu_N/(Sm_N \times Gd_N)^{1/2}$; N, REE are normalized by Upper Continental Crust (UCC) [26].

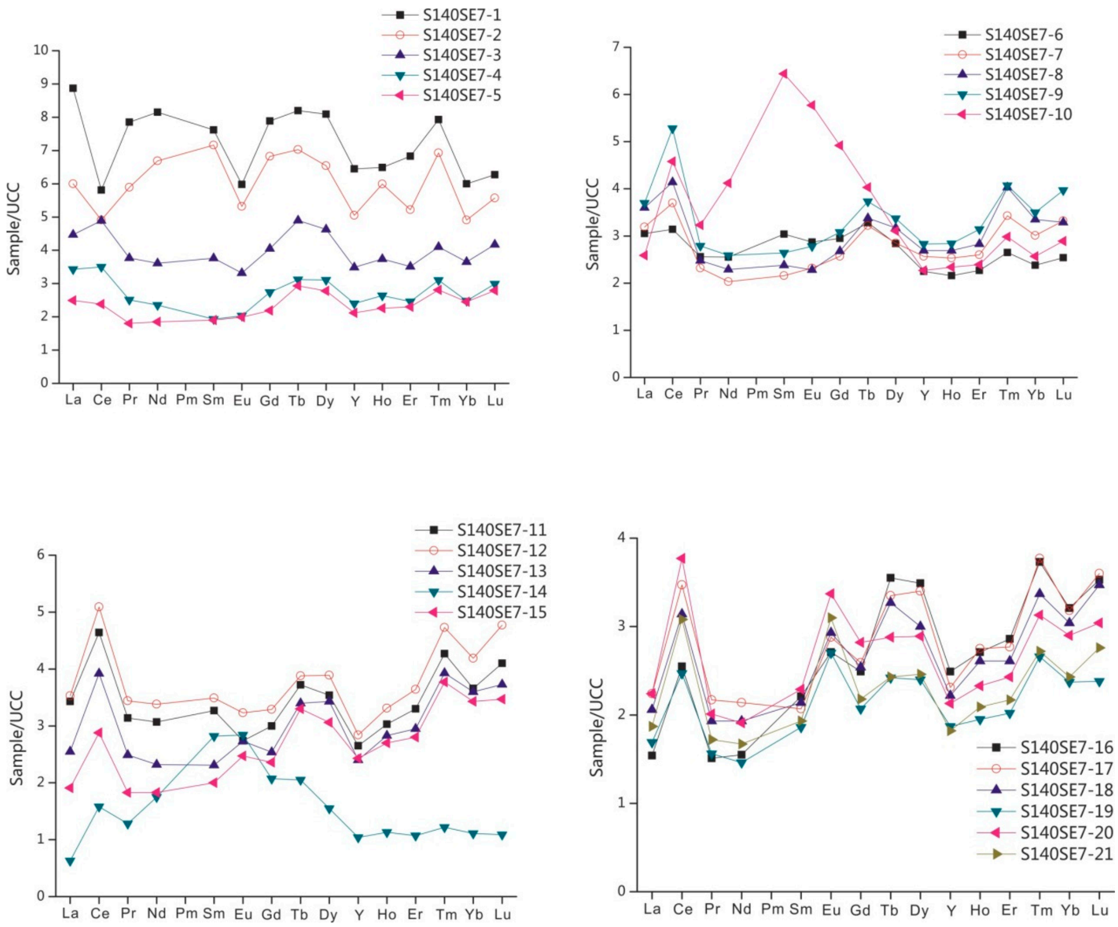

Figure 7. Distribution patterns of REE in the tuff samples from Zhongliangshan mine. REE are normalized by Upper Continental Crust [26].

Two reasons may be responsible for the H-REE enrichment of the tuff samples in the Zhongliangshan mine. First, L-REE can be easily leached by groundwater than H-REE; Second, L-REE can be easily adsorbed on the organic matter than the H-REE [37], which may be adsorbed by the coal seam overlying the tuff. The REE enrichment mode in the Zhongliangshan tuff is similar to that of Songzao Coalfield. Some studies have shown that L-REE are more easily to be leached by groundwater and are more apt to be adsorbed by organic matter [38–42].

5. Discussion

5.1. Origin of Tuff

In the late Permian Age, the Dongwu movement, one of the most important tectonic events in southern China, caused the upper Yangtze basin uplifting and the subsequent sea regression, which led to an extensive erosion in the area. The upper part of Maokou limestone of Sichuan Basin had been subjected to a serious erosion, resulting in the formation of a vast weathering residual plain, where peat subsequently accumulated. Meanwhile, the Emeishan basalt volcano began erupting and reached a climax in the early stage of late Permian, leading to a tuff layer overlying the Maokou limestone [17].

Al_2O_3 and TiO_2 are both stable components in the rock and would be little altered during alteration, so the ratio of TiO_2/Al_2O_3 (KAT) would be kept constant and can frequently be used to study the origin of volcanic ash [29,42]. It is suggested that KAT values for silicic volcanic ash are <0.02, and those for mafic and alkali volcanic ashes are >0.08 and between 0.02 and 0.08, respectively [43,44]. The KAT ratios of the tuff in the Zhongliangshan mine are >0.08 (Figure 8), suggesting a mafic volcanic origin. In addition, the tuff samples fall in the area basalt to alkali basalt from the La/Yb-REE diagram (Figure 9), indicating a feature of alkali basalt.

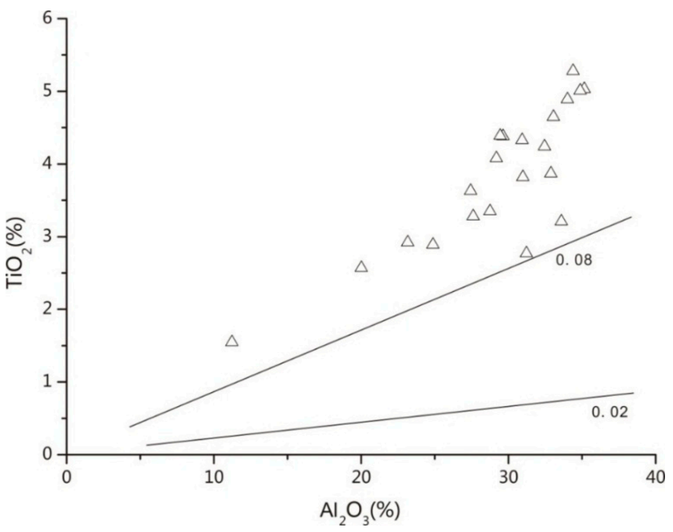

Figure 8. Plot for TiO_2 *vs.* Al_2O_3 of tuff samples in the Zhongliangshan mine, Chongqing.

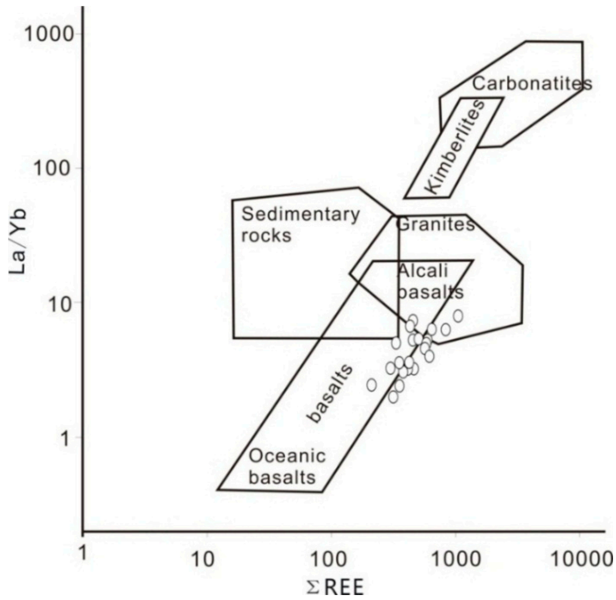

Figure 9. Relation between REE and La/Yb of tuff samples in the Zhongliangshan mine, Chongqing.

5.2. Hydrothermal Solution

Some researchers have shown that there have been activities of low-temperature hydrothermal solutions in the late Permian Age in southwestern China, which resulted in enrichment of trace elements and minerals in some coal [1,45–51]. Similarly, some minerals of tuff in Zhongliangshan are formed owing to the influence of hydrothermal solution.

In addition to the derivation from volcanic ash, anatase and zircon might have been derived from hydrothermal alteration in the Zhongliangshan tuffs. Anatase of various particle sizes is distributed in the kaolinite matrix (Figure 4B,C). Figures 4A and 5A illustrate that part of anatase could be formed by hydrothermal alteration. Zircon from Figure 5D displays long axis and could be formed by the effect of hydrothermal alteration. Zircon in Figure 5D exclusively contains Zr, Si and O determined by the SEM-EDX. Finkelman [52] has demonstrated that Hf, Th, U, Y and HREE occur in the volcanogenic zircon, but were not identified in authigenic ziron, in accordance with the results of the Zhongliangshan tuff samples.

Florencite, the main carrier of REE in the Zhongliangshan tuff samples, occurs as ellipsoidal in the kaolinite matrix (Figure 5E,F), indicating a syngenetic or early diagenetic hydrothermal origin. Dai *et al.* [14] have also demonstrated that florencite is one of the important carriers of REE in the late Permian coals in southwestern China [3].

Gypsum (Figure 5B) and barite (Figure 4F) occur as crack-fillings, the former occurring as radiating and the latter on the edge of jarosite, indicating an epigenetic hydrothermal origin.

5.3. Preliminary Evaluation of Rare Metals

Coal and coal-bearing strata have recently become alternative sources for recovery of rare metals [2,3,7,8]. The U.S. Department of Energy's National Energy Technology Laboratory has selected 10 projects to receive funding for research in support of the lab's program on recovery of rare earth elements from coal and coal byproducts since 2015 [2,53].

Based on the Chinese industry standards [33], the required $(Nb,Ta)_2O_5$ concentrations for marginal and industrial grade Nb(Ta) ore deposits of weathered crust type are 80–100 and 160–200 μg/g, respectively; equivalent concentrations are 40–60 and 100–120 μg/g for Nb(Ta) ore deposits of river placer type. The concentration of $(Nb,Ta)_2O_5$ varies from 47 to 324 μg/g, with an average of 186 μg/g, higher than the marginal and industrial grade for weathered crust and placer deposit types. Concentration of TiO_2 varies from 1.55% to 5.28% and averages 3.82%, higher than the industrial grade of Chinese industry standard [54]. The average concentration of Ga (38.2 μg/g) is also up to the standards for industrial utilization in bauxite (20 μg/g) and coal mining (30 μg/g) [34]. In addition, the concentrations of REE vary from 234 to 1189 μg/g and averages 548 μg/g, higher than the cut-off grade of Chinese weathering crust ion adsorption type rare earth elements deposits (500 μg/g) [55].

The Nb, Ti, Ga, and REE all exceed their respective industrial grade of China in the tuff of the Zhongliangshan mine. It is considered that the Zhongliangshan tuff is a potential polymetallic ore worth in-depth study.

6. Conclusions

Compared with the Upper Continental Crust, some trace elements including Li, Be, Sc, V, Cr, Co, Ni, Cu, Zn, Ga, Zr, Nb, Cd, Sb, REE, Hf, Ta, Re, Th, and U are enriched in tuff from Zhongliangshan mine, Chongqing, southwestern China. The minerals mainly include kaolinite, illite, pyrite, anatase, calcite, gypsum, quartz, and traces of minerals such as zircon, florencite, jarosite, and barite. The tuff is of mafic volcanic origin with features of alkali basalt. The H-REE enriched in the tuff due to L-REE being leached easier by groundwater and adsorbed in the organic matter of the coal seam overlying the tuff. Some minerals including florencite, gypsum, barite, and a portion of anatase and zircon are precipitated from hydrothermal solution. It is suggested that Zhongliangshan tuff is a potential polymetallic ore and the opportunity for recovery of these valuable elements needs to be studied in depth.

Acknowledgments: The authors wish to express their appreciation to Shifeng Dai for revision suggestions and English polishing. We thank Lei Zhao and Lixin Zhao, who helped to identify the minerals under SEM-EDX. We also thank Peipei Wang for the mineral quantitative analysis using Siroquant software. The authors are indebted to three anonymous reviewers for their careful reviews and constructive comments, which greatly improved the manuscript. This research was supported by the National Key Basic Research and Development Program (No.2014CB238902) and National Natural Science Foundation of China (No. 41502162).

Author Contributions: Jianhua Zou and Heming Tian collected tuff samples in Zhongliangshan mine. Jianhua Zou conducted the determinations of major-element contents. Tian Li and Heming Tian were responsible for the analysis of trace-element concentrations. Jianhua Zou and Tian Li were responsible for the mineralogy investigation using XRD and SEM-EDX.

Conflicts of Interest: The authors declare no conflict of interest.

References

1. Dai, S.F.; Ren, D.Y.; Chou, C.-L.; Finkelman, R.B.; Seredin, V.V.; Zhou, Y.P. Geochemistry of trace elements in Chinese coals: A review of abundances, genetic types, impacts on human health, and industrial utilization. *Int. J. Coal Geol.* **2012**, *94*, 3–21. [CrossRef]
2. Hower, J.C.; Granite, E.J.; Mayfield, D.B.; Lewis, A.S.; Finkelman, R.B. Notes on Contributions to the Science of Rare Earth Element Enrichment in Coal and Coal Combustion Byproducts. *Minerals* **2016**, *6*, 32. [CrossRef]
3. Dai, S.F.; Chekryzhov, I.Y.; Seredin, V.V.; Nechaev, V.P.; Graham, I.T.; Hower, J.C.; Ward, C.R.; Ren, D.Y.; Wang, X.B. Metalliferous coal deposits in East Asia (Primorye of Russia and South China): A review of geodynamic controls and styles of mineralization. *Gondwana Res.* **2016**, *29*, 60–82. [CrossRef]
4. Dai, S.F.; Wang, P.P.; Ward, C.R.; Tang, Y.G.; Song, X.L.; Jiang, J.H.; Hower, J.C.; Li, T.; Seredin, V.V.; Wagner, N.J.; *et al.* Elemental and mineralogical anomalies in the coal-hosted Ge ore deposit of Lincang, Yunnan, southwestern China: Key role of N_2-CO_2-mixed hydrothermal solutions. *Int. J. Coal Geol.* **2015**, *152*, 19–46. [CrossRef]
5. Johnston, M.N.; Hower, J.C.; Dai, S.; Wang, P.; Xie, P.; Liu, J. Petrology and Geochemistry of the Harlan, Kellioka, and Darby Coals from the Louellen 7.5-Minute Quadrangle, Harlan County, Kentucky. *Minerals* **2015**, *5*, 894–918. [CrossRef]
6. Seredin, V.V.; Finkelman, R.B. Metalliferous coals: A review of the main genetic and geochemical types. *Int. J. Coal Geol.* **2008**, *76*, 253–289. [CrossRef]
7. Seredin, V.V.; Dai, S.F. Coal deposits as potential alternative sources for lanthanides and yttrium. *Int. J. Coal Geol.* **2012**, *94*, 67–93. [CrossRef]
8. Seredin, V.V.; Dai, S.F.; Sun, Y.Z.; Chekryzhov, I.Y. Coal deposits as promising sources of rare metals for alternative power and energy-efficient technologies. *Appl. Geochem.* **2013**, *31*, 1–11. [CrossRef]
9. Dai, S.F.; Seredin, V.V.; Ward, C.R.; Jiang, J.H.; Hower, J.C.; Song, X.L.; Jiang, Y.F.; Wang, X.B.; Gornostaeva, T.; Li, X.; *et al.* Composition and modes of occurrence of minerals and elements in coal combustion products derived from high-Ge coals. *Int. J. Coal Geol.* **2014**, *121*, 79–97. [CrossRef]
10. Seredin, V.V. From coal science to metal production and environmental protection: A new story of success. *Int. J. Coal Geol.* **2012**, *90–91*, 1–3. [CrossRef]
11. Dai, S.F.; Zhou, Y.P.; Zhang, M.Q.; Wang, X.B.; Wang, J.M.; Song, X.L.; Jiang, Y.F.; Luo, Y.B.; Song, Z.T.; Yang, Z.; *et al.* A new type of Nb (Ta)–Zr(Hf)–REE–Ga polymetallic deposit in the late Permian coal-bearing strata, eastern Yunnan, southwestern China: Possible economic significance and genetic implications. *Int. J. Coal Geol.* **2010**, *83*, 55–63. [CrossRef]
12. Dai, S.F.; Seredin, V.V.; Ward, C.R.; Hower, J.C.; Xing, Y.W.; Zhang, W.G.; Song, W.J.; Wang, P.P. Enrichment of U-Se-Mo-Re-V in coals preserved within marine carbonate successions: Geochemical and mineralogical data from the Late Permian Guiding Coalfield, Guizhou, China. *Miner. Deposita* **2015**, *50*, 159–186. [CrossRef]
13. Hower, J.C.; Eble, C.F.; O'Keefe, J.M.K.; Dai, S.F.; Wang, P.P.; Xie, P.P.; Liu, J.J.; Ward, C.R.; French, D. Petrology, Palynology, and Geochemistry of Gray Hawk Coal (Early Pennsylvanian, Langsettian) in Eastern Kentucky, USA. *Minerals* **2015**, *5*, 592–622. [CrossRef]
14. Dai, S.F.; Zhao, L.; Hower, J.C.; Johnston, M.N.; Song, W.J.; Wang, P.P.; Zhang, S.F. Petrology, mineralogy, and chemistry of size-fractioned fly ash from the Jungar power plant, Inner Mongolia, China, with emphasis on the distribution of rare earth elements. *Energy Fuels* **2014**, *28*, 1502–1514. [CrossRef]
15. Zhuang, X.G.; Su, S.C.; Xiao, M.G.; Li, J.; Alastuey, A.; Querol, X. Mineralogy and geochemistry of the Late Permian coals in the Huayingshan coal-bearing area, Sichuan Province, China. *Int. J. Coal Geol.* **2012**, *94*, 271–282. [CrossRef]
16. Dai, S.F.; Yang, J.Y.; Ward, C.R.; Hower, J.C.; Liu, H.D.; Garrison, T.M.; French, D.; O'Keefe, J.M.K. Geochemical and mineralogical evidence for a coal-hosted uranium deposit in the Yili Basin, Xinjiang, northwestern China. *Ore Geol. Rev.* **2015**, *70*, 1–30. [CrossRef]
17. China Coal Geology Bureau. *Sedimentary Environments and Coal Accumulation of Late Permian Coal Formation in Western Guizhou, Southern Sichuan and Eastern Yunnan, China*; Chongqing University Press: Chongqing, China, 1996. (In Chinese).
18. Dai, S.F.; Liu, J.J.; Ward, C.R.; Hower, J.C.; French, D.; Jia, S.H.; Hood, M.M.; Garrison, T.M. Mineralogical and geochemical compositions of Late Permian coals and host rocks from the Guxu Coalfield, Sichuan Province, China, with emphasis on enrichment of rare metals. *Int. J. Coal Geol.* **2016**. [CrossRef]

19. Standardization Administration of the People's Republic of China. *Sampling of Coal Seams*; Chinese Standard GB/T 482–2008. Standardization Administration of the People's Republic of China: Beijing, China, 2008. (In Chinese)
20. ASTM International. *Test Method for Ash in the Analysis Sample of Coal and Coke from Coal*; ASTM D3174–11; ASTM International: West Conshohocken, PA, USA, 2011.
21. Taylor, J.C. Computer programs for standardless quantitative analysis of minerals using the full powder diffraction profile. *Powder Diffr.* **1991**, *6*, 2–9. [CrossRef]
22. Rietveld, H.M. A profile refinement method for nuclear and magnetic structures. *Appl. Crystallogr.* **1969**, *2*, 65–71. [CrossRef]
23. Ward, C.R.; Spears, D.A.; Booth, C.A.; Staton, I.; Gurba, L.W. Mineral matter and trace elements in coals of the Gunnedah Basin, New South Wales, Australia. *Int. J. Coal Geol.* **1999**, *40*, 281–308.
24. Ward, C.R.; Matulis, C.E.; Taylor, J.C.; Dale, L.S. Quantification of mineral matter in the Argonne Premium coals using interactive Rietveld-based X-ray diffraction. *Int. J. Coal Geol.* **2001**, *46*, 67–82. [CrossRef]
25. Ruan, C.D.; Ward, C.R. Quantitative X-ray powder diffraction analysis of clay minerals in Australian coals using Rietveldmethods. *Appl. Clay Sci.* **2002**, *21*, 227–240. [CrossRef]
26. Taylor, S.R.; McLennan, S.M. *The Continental Crust: Its Composition and Evolution*; Blackwell: Oxford, UK, 1985; p. 312.
27. Chi, Q.H.; Yan, M.C. *Handbook of Elemental Abundance for Applied Geochemistry*; Geological Publishing House: Beijing, China, 2007; pp. 1–148. (In Chinese)
28. Zhou, Y.P.; Ren, Y.L. Element gochemistry of volcanic ash derived tonsteins in late Permian coal-bearing formation of eastern Yunnan and western Guizhou, China. *Acta Sedimentol Sin.* **1994**, *12*, 123–132. (In Chinese)
29. Zhou, Y.P.; Bohor, B.F.; Ren, Y.L. Trace element geochemistry of altered volcanic ash layers (tonsteins) in late Permian coal-bearing formations of eastern Yunnan and western Guizhou provinces, China. *Int. J. Coal Geol.* **2000**, *44*, 305–324. [CrossRef]
30. Sichuan Bureau of Coal Geology; Sichuan Institute of Coal Geology. *Sedimentary Environment and Coal Accumulating Regulations of Late Permian Coal-Bearing Formation in Southern Sichuan*; Guizhou Sceinece and Technology Press: Guiyang, China, 1994. (In Chinese)
31. Dai, S.F.; Chou, C.-L.; Yue, M.; Luo, K.L.; Ren, D.Y. Mineralogy and geochemistry of a Late Permian coal in the Dafang Coalfield, Guizhou, China: Influence from siliceous and iron-rich calcic hydrothermal fluids. *Int. J. Coal Geol.* **2005**, *61*, 241–258. [CrossRef]
32. Dai, S.F.; Ren, D.Y.; Zhou, Y.P.; Chou, C.-L.; Wang, X.B.; Zhao, L.; Zhu, X.W. Mineralogy and geochemistry of a superhigh-organic-sulfur coal, Yanshan Coalfield, Yunnan, China: Evidence for a volcanic ash component and influence by submarine exhalation. *Chem. Geol.* **2008**, *255*, 182–194. [CrossRef]
33. DZ/T 0203–2002. *Geology Mineral Industry Standard of P.R. China: Specifications for Rare Metal Mineral Exploration*; Geological Press: Beijing, China, 2002. (In Chinese)
34. Mineral Resources Industry Requirements Manual Editorial Board. *Mineral Resources Industry Requirements Manual*; Geological Press: Beijing, China, 2010. (In Chinese)
35. Dai, S.F.; Graham, I.T.; Chou, C.-L.; Ward, C.R. A review of anomalous rare earth elements and yttrium in coal. *Int. J. Coal Geol.* **2016**, *159*, 82–95. [CrossRef]
36. Bao, Z.W.; Zhao, Z.H. Geochemistry of mineralization with exchangeable REY in the weathering crusts of granitic rocks in South China. *Ore Geol. Rev.* **2008**, *33*, 519–535. [CrossRef]
37. Dai, S.F.; Li, D.; Chou, C.-L.; Zhao, L.; Zhang, Y.; Ren, D.Y.; Ma, Y.W.; Sun, Y.Y. Mineralogy and geochemistry of boehmite-rich coals: New insights from the Haerwusu Surface Mine, Jungar Coalfield, Inner Mongolia, China. *Int. J. Coal Geol.* **2008**, *74*, 185–202. [CrossRef]
38. Eskenazy, G.M. Rare earth elements in a sampled coal from the Pirin Deposit, Bulgaria. *Int. J. Coal Geol.* **1987**, *7*, 301–314. [CrossRef]
39. Crowley, S.S.; Stanton, R.W.; Ryer, T.A. The effects of volcanic ash on the maceral and chemical composition of the C coal bed, Emery Coal Field, Utah. *Org. Geochem.* **1989**, *14*, 315–331. [CrossRef]
40. Hower, J.C.; Ruppert, L.F.; Eble, C.F. Lanthanide, yttrium, and zirconium anomalies in the fire Clay coal bed, Eastern Kentucky. *Int. J. Coal Geol.* **1999**, *39*, 141–153. [CrossRef]
41. Dai, S.F.; Ren, D.Y.; Chou, C.-L.; Li, S.S.; Jiang, Y.F. Mineralogy and geochemistry of the No. 6 coal (Pennsylvanian) in the Jungar Coalfield, Ordos Basin, China. *Int. J. Coal Geol.* **2006**, *66*, 253–270. [CrossRef]

42. Dai, S.F.; Li, T.J.; Jiang, Y.F.; Ward, C.R.; Hower, J.C.; Sun, J.H.; Liu, J.J.; Song, H.J.; Wei, J.P.; Li, Q.Q.; *et al.* Mineralogical and geochemical compositions of the Pennsylvanian coal in the Hailiushu Mine, Daqingshan Coalfield, Inner Mongolia, China: Implications of sediment-source region and acid hydrothermal solutions. *Int. J. Coal Geol.* **2015**, *137*, 92–110. [CrossRef]
43. Addison, R.; Harrison, R.K.; Land, D.H.; Young, B.R.; Davis, A.E.; Smith, T.K. Volcanogenic tonsteins from tertiary coal measures, East Kalimantan, Indonesia. *Int. J. Coal Geol.* **1983**, *3*, 1–30. [CrossRef]
44. Burger, K.; Zhou, Y.P.; Ren, D.Y. Petrography and geochemistry of tonsteins from the 4th Member of the Upper Triassic Xujiahe Formation in southern Sichuan Province, China. *Int. J. Coal Geol.* **2002**, *49*, 1–17. [CrossRef]
45. Dai, S.F.; Zhang, W.G.; Seredin, V.V.; Ward, C.R.; Hower, J.C.; Song, W.J.; Wang, X.B.; Li, X.; Zhao, L.; Kang, H.; *et al.* Factors controlling geochemical and mineralogical compositions of coals preserved within marine carbonate successions: A case study from the Heshan Coalfield, southern China. *Int. J. Coal Geol.* **2013**, *109–110*, 77–100. [CrossRef]
46. Dai, S.F.; Zhang, W.G.; Ward, C.R.; Seredin, V.V.; Hower, J.C.; Li, X.; Song, W.J.; Wang, X.B.; Kang, H.; Zheng, L.C.; *et al.* Mineralogical and geochemical anomalies of Late Permian coals from the Fusui Coalfield, Guangxi Province, southern China: Influences of terrigenous materials and hydrothermal fluids. *Int. J. Coal Geol.* **2013**, *105*, 60–84. [CrossRef]
47. Ren, D.Y.; Zhao, F.H.; Dai, S.F.; Zhang, J.Y.; Luo, K.L. *Geochemistry of Trace Elements in Coal*; Science Press: Beijing, China, 2006. (In Chinese)
48. Zhou, Y.P.; Ren, Y.L. Distribution of arsenic in coals of Yunnan Province, China, and its controlling factors. *Int. J. Coal Geol.* **1992**, *20*, 85–98. [CrossRef]
49. Dai, S.F.; Chou, C.-L. Occurrence and origin of minerals in a chamosite-bearing coal of Late Permian age, Zhaotong, Yunnan, China. *Am. Mineral.* **2007**, *92*, 1253–1261. [CrossRef]
50. Wang, X.B.; Dai, S.F.; Chou, C.-L.; Zhang, M.Q.; Wang, J.M.; Song, X.L.; Wang, W.; Jiang, Y.F.; Zhou, Y.P.; Ren, D.Y. Mineralogy and geochemistry of Late Permian coals from the Taoshuping Mine, Yunnan Province, China: Evidences for the sources of minerals. *Int. J. Coal Geol.* **2012**, *96–97*, 49–59. [CrossRef]
51. Dai, S.F.; Tian, L.W.; Chou, C.-L.; Zhou, Y.P.; Zhang, M.Q.; Zhao, L.; Wang, J.M.; Yang, Z.; Cao, H.Z.; Ren, D.Y. Mineralogical and compositional characteristics of Late Permian coals from an area of high lung cancer rate in Xuan Wei, Yunnan, China: Occurrence and origin of quartz and chamosite. *Int. J. Coal Geol.* **2008**, *76*, 318–327. [CrossRef]
52. Finkelman, R.B. *Modes of Occurrence of Trace Elements in Coal*; US Geological Survey Open-File Report; United States Geological Survey: Reston, VA, USA, 1981; No. 81–99; p. 322.
53. The U.S. Department of Energy. Available online: http://www.energy.gov/fe/articles/doe-selects-projects-enhance-its\T1\textquoterights-research-recovery-rare-earth-elements-coal-and-coal.2015 (accessed on 2 December 2015).
54. DZ/T 0208–2002. *Geology Mineral Industry Standard of P.R. China: Specifications for Placer (Metallic Mineral) Exploration*; Geological Press: Beijing, China, 2002. (In Chinese)
55. DZ/T 0204–2002. *Geology Mineral Industry Standard of P.R. China: Specifications for Rare Earth Mineral Exploration*; Geological Press: Beijing, China, 2002. (In Chinese)